

Article

# Characterisation of NiTi Orthodontic Archwires Surface after the Simulation of Mechanical Loading in CACO2-2 Cell Culture

Nikola Lepojević <sup>1</sup>, Ivana Šćepan <sup>1</sup> , Branislav Glišić <sup>1</sup>, Monika Jenko <sup>2</sup>, Matjaž Godec <sup>2</sup>, Samo Hočevar <sup>3</sup> and Rebeka Rudolf <sup>4,\*</sup> 

<sup>1</sup> Department of Orthodontics, School of Dental Medicine, University of Belgrade, Doktora Subotića 8, 11000 Belgrade, Serbia

<sup>2</sup> Department of Surface Physics and Chemistry of Materials, Institute of Metals and Technology, Lepi pot 11, 1000 Ljubljana, Slovenia

<sup>3</sup> Department of Analytical Chemistry, National Institute of Chemistry, Hajdrihova 19, 1001 Ljubljana, Slovenia

<sup>4</sup> Faculty of Mechanical Engineering, University of Maribor, Smetanova 17, 2000 Maribor, Slovenia

\* Correspondence: rebeka.rudolf@um.si

Received: 17 June 2019; Accepted: 10 July 2019; Published: 15 July 2019



**Abstract:** Nickel-titanium (NiTi) orthodontic archwires are crucial in the initial stages of orthodontic therapy when the movement of teeth and deflection of the archwire are the largest. Their great mechanical properties come with their main disadvantage—the leakage of nickel. Various in vitro studies measured nickel leakage from archwires that were only immersed in the medium with little or minimal simulation of all stress and deflection forces that affect them. This study aims to overcome that by simulating deflection forces that those archwires are exposed to inside the mouth of a patient. NiTi orthodontic archwires were immersed in CACO2-2 cell culture medium and then immediately loaded while using a simulator of multiaxial stress for 24 h. After the experiment, the surface of the NiTi orthodontic archwires were analysed while using scanning electron microscopy (SEM) and auger electron spectroscopy (AES). The observations showed significant microstructural and compositional changes within the first 51 nm thickness of the archwire surface. Furthermore, the released nickel and titanium concentrations in the CACO2-2 cell culture medium were measured while using Inductively Coupled Plasma Mass Spectroscopy (ICP-MS). It was found out that the level of released nickel ions was 1.310 µg/L, which can be assigned as statistically significant results. These data represent the first mention of the already detectable release of Ni ions after 24 h during the simulation of mechanical loading in the CACO2-2 cell culture medium, which is important for clinical orthodontic praxis.

**Keywords:** nickel-titanium; orthodontic archwires; surface; simulation; mechanical loading; CACO2-2 cell culture medium; scanning electron microscopy (SEM); auger electron spectroscopy (AES); inductively coupled plasma mass spectroscopy (ICP-MS)

## 1. Introduction

Today, shape memory alloys (SMA) have a wide variety of medical applications, including dentistry, especially for orthodontic treatment. They are attractive due to their superelasticity behaviour or functional property above the temperature austenite finish ( $A_f$ ), and they are characterised by martensitic phase transformation, which is caused by the initiation of stress with enough value, leading to the changes of phase or microstructure in the SMA (austenite to martensite). Nickel-titanium (NiTi) orthodontic archwires are the most useful, where nickel and titanium are in equiatomic proportions—they are known as Nitinol. An ongoing challenge in the design of NiTi orthodontic archwires is to simultaneously have excellent biocompatibility, while also retaining adequate mechanical

properties. The biocompatibility of NiTi orthodontic archwires has been investigated in many different studies [1–11]. Clinicians remain cautious of NiTi orthodontic archwire usage, because of their large nickel content, a long period of time being required for orthodontic treatment, and the high incidence of allergic reactions to nickel [1]. Several case reports describe allergic reactions of orthodontic patients to NiTi archwires [2,3]. One study concluded that there may be a risk of sensitising patients to nickel after long-term exposure [4]. Many studies proved the cytotoxicity of nickel, as it reduced the level of glutathione by binding to the sulfhydryl group of amino acids [5,6]. Nickel may also cause: lymphotoxicity [7], immunotoxicity [8], haemotoxicity [9], genotoxicity [10], and carcinogenicity [11]. Many studies have demonstrated that nickel release from these wires is very low and under the required threshold to cause biological effects, despite the high content of nickel in NiTi archwires [12–14]. The reason for this is that NiTi archwires have a high content of titanium, which makes it possible to form, with Ni, a stable crystal lattice with minimal potential release of nickel ions during the orthodontic treatment. On the other hand, titanium is a highly reactive element, which, once in contact with oxygen, immediately reacts to form a titanium oxide layer on the surface of the alloy. It is mainly composed of  $TiO_2$  as the free enthalpy of formation of  $TiO_2$  is negative, and it exceeds the enthalpy of the formation of nickel oxides by at least two- or three-fold in absolute value [15]. It protects the archwires from corrosion, and it creates a physical and mechanical barrier for the oxidation of nickel, leaving it deeper in the archwire [16]. This titanium oxide layer is very passive, but it could be removed or destroyed by many different factors in the mouth. Those archwires are under constant mechanical stress in the mouth, and they are simultaneously immersed in saliva, ingested fluids, temperature fluctuations, masticatory force, and topical fluoride modalities (toothpaste, mouthwashes, gels and varnish) [17], which also affect the surface of the archwires. Besides this, titanium has one great disadvantage, i.e., poor tribological properties and it exhibits high friction and wear coefficients, as well as poor abrasion and fretting resistance when sliding against itself or other material [18]. Inside the mouth, the NiTi archwires are in constant contact with brackets that are made from different materials (stainless steel, ceramic, composite). Constant sliding and friction is inevitable in between them. Additionally, oxides, impurities, and pores are the key reasons for severe cavitation erosion damage of the NiTi [19].

Many *in vitro* studies examined NiTi archwires in static environments by putting them in different media and determining the level of released nickel [20,21]. Some experimental research deformed NiTi archwires only using one-dimensional loading, or failed to deform them at all. These procedures displayed results, whereby the level of released nickel showed little correspondence to the nickel that was released in the mouth. The Orthodontists deform NiTi archwire during the therapy and place it inside the bracket slot of every tooth (as shown in Figure 1a). The main stresses that deform NiTi archwires are the combination of bending stresses (tension and compressive) in conjunction with torsion and bending stresses. Archwires start unloading in order to come into a more stable austenitic phase and produce forces that move teeth after being placed inside the brackets. Teeth will move in a different manner, depending on the various levels of periodontal loss and the different stress distribution inside a healthy, endodontically treated, and restored tooth [22]. Fercec et al. [23] designed the simulation of multiaxial stress equipment (SMAS) that could provide uniaxial and multiaxial forces in order to deform the NiTi archwires (Figure 1b). With SMAS, different mechanical loading of the archwires can be simulated to imitate the real situation in the oral cavity. It is necessary to emphasize here that SMAS can only simulate intraoral forces that originate from the crowding of the teeth and the bending angle of the archwire, and cannot simulate frictional or masticatory forces. Based on the literature review, it was found that the experiment was not created to simulate contact of any fluid (medium) from the mouth with the archwires under loading. Consequently, the SMAS needed to be altered to facilitate contact of the NiTi archwires with the proper medium.

Based on this thesis, our research focused on the immersion of NiTi orthodontic archwires in medium and loading immediately, while using the SMAS for 24 h at an ambient temperature. The CACO2-2 cell culture medium was chosen, because it represents heterogeneous cells and it has

found applications in cell invasion studies. The CACO-2 cell culture medium is used widely across the pharmaceutical industry as an *in vitro* model of the human small intestinal mucosa to predict the absorption of orally administered drugs with different kits [24]. Consequently, all of the metals that were released into the mouth of a patient during orthodontic treatment reach the intestines and CACO-2 cells as its crucial part. Various studies proved that nickel [25] and TiO<sub>2</sub> nanoparticles affect CACO-2 cells [26,27]. Those metals caused changes in cell viability, protein synthesis, geno-toxicity, oxidative stress,  $\beta$ -actin synthesis, and gene expression. All of those effects of nickel on cells were observed during 24 h, as in our study. The selected time, 24 h of simulation test, was chosen in accordance with the findings by Staffolani et al. [28], who discovered that nickel release from archwires reached its highest values on the first day. Some studies even point out that the initial Ni release increases are sustained, and they fail to drop over a prolonged period of a few months [29–32]. The amount of nickel that is released can vary, depending on the variable nickel surface concentrations that were reported for NiTi archwires (0.4–15 at.%) [33]. After the testing, demanding investigations were carried out, including the observation of changes on the NiTi orthodontic archwires' surface and measuring the ions' content in CACO-2 cell culture medium as the results of release from the archwires. The logic of measuring the level of nickel in the CACO-2 cell line, instead of using the keratocytes, was that nickel released from the orthodontic archwire only stays a short amount of time in the mouth of a patient. It is ingested and, therefore, stays a much longer time in the colon, where it has higher chances to interact and affect cells. Similar, like in Pagano et al.' study [34], the cytotoxicity essay (MTT-3-(4,5-dimethylthiazol-2-yl)-2,5-diphenyltetrazolium bromide reduction assay) was planned to be done on CACO-2 cell culture, and to determine cell viability according to mitochondrial enzyme dehydrogenase activity.

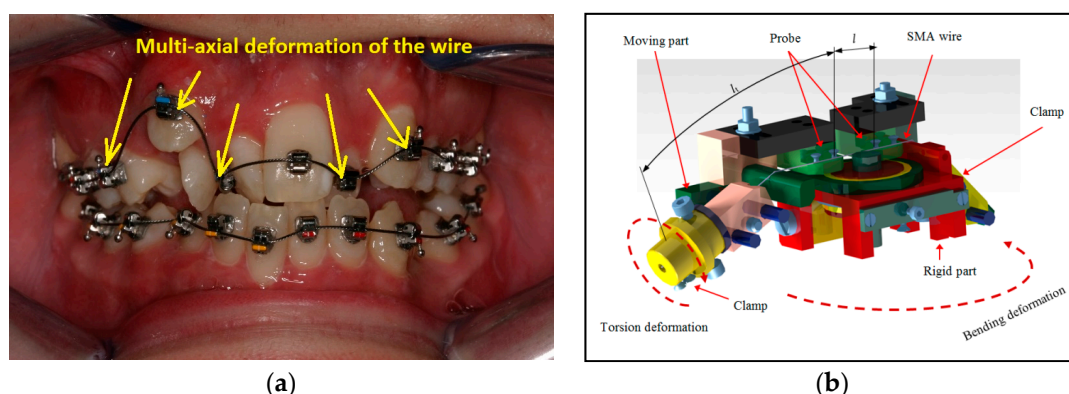


**Figure 1.** (a) Fixed orthodontic appliance (arrow pointing to the bending and torsional stresses of the archwire); (b) Simulation of multi-axial stress equipment (SMAS) [23]. Reprinted with permission from [23]. © 2014 Elsevier.

The aim of this work was to discover any changes in the surface of NiTi archwires and, if they are present, to measure the surface concentration of elements and released ion content into the medium during a 24 h deflection time. The null hypotheses of this study were: (1) There are no changes in the concentration of elements in the 51 nm of the wire surface, (2) A significant amount of nickel is not released from the wires into the medium, and (3) The amount of released nickel is the same for the deformed and initial archwires.

## 2. Materials and Methods

### 2.1. Materials

Commercially available NiTi archwires Rematitan (Dentaurum, Ispringen, Germany) dimensions 0.40 mm  $\times$  0.56 mm (0.016"  $\times$  0.022") were used in this study. The selected archwires had nearly equiatomic composition (50 at.% Ni, 50 at.% Ti). The American Type Culture Collection provided the

CACO-2 cell line (ATCC, Manassas, VA, USA) and it represented a continuous heterogeneous human epithelial colorectal adenocarcinoma cell line.

## 2.2. Methods

Mechanical loading in CACO2-2 cell culture SMAS was used for the simulation of NiTi orthodontic archwires [23] with the reconstruction, which represents the additional installation of a chamber (Figure 2a,b) with the volume 4 mL. The chamber was made from polymer material (plexiglass), which exhibits excellent mechanical and dimensional stability, and it is highly inert. It also lacks any metal that could contaminate the results, and it is not electro-conductive. The chamber construction was created, so that the CACO2-2 cell culture medium was in continuous contact with the archwires during testing in the SMAS: The archwires that were inside the SMAS went through the chamber in one part of their length. The chamber was closed with a cover that was made from the same material as the chamber to prevent leaking and evaporation of the liquid. Evaporation was prevented using the cover, which was further surrounded by silicone to entirely seal the chamber, therefore that amount of medium could be placed inside it during the experiment. For the purpose of this study, the archwires were immersed in CACO-2 cell culture medium inside the chamber.

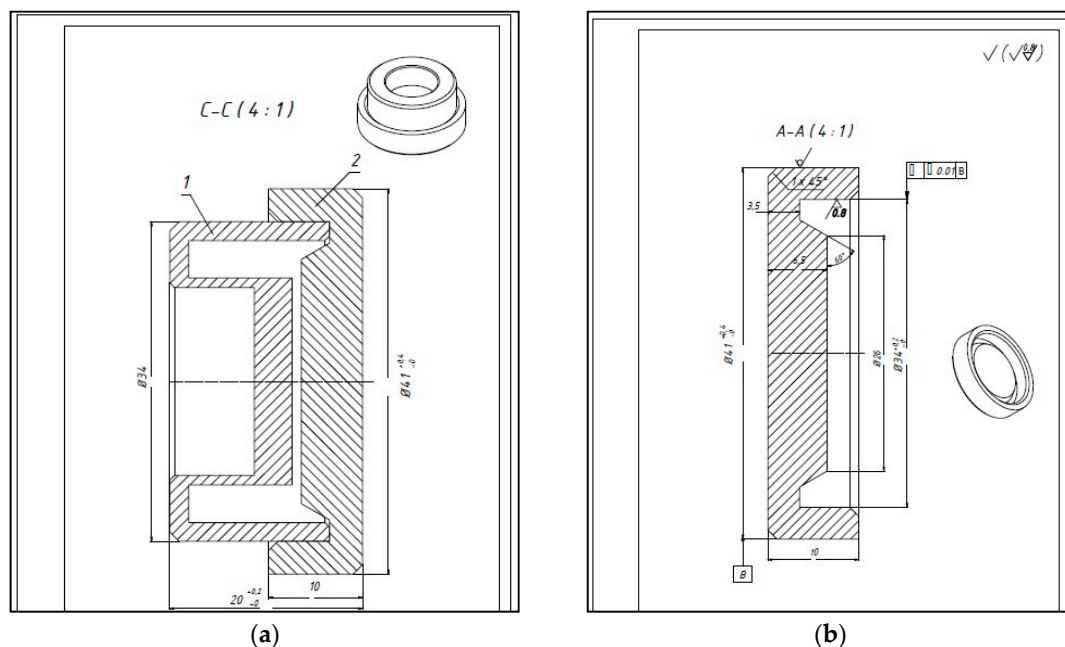


**Figure 2.** Schematic presentation of (a) the chamber and (b) the cover.

## 2.3. Experimental Setup

In the simulation testing, orthodontic archwires Rematitan (Dentaurum, Ispringen, Germany) were placed in the SMAS (National Instruments OM 21 benchtop micro-ohmmeter, AOIP company, 52 Avenue Paul Langevin, 91130 Ris-Orangis, Paris, France) through the chamber and then bent at an angle of  $30^\circ$ , which represents the mean bending angle in the mouth of the average orthodontic patient. The length of the archwire in contact with CACO-2 cell culture medium was 3 cm. Four archwires were placed into the SMAS chamber at the same time in order to get as close to the situation of an average orthodontic patient, where about 12–15 cm length of orthodontic archwire is needed. After this, 4 mL of CACO-2 cell culture medium was added to the chamber and, in the next phase, the simulation test started for 24 h. A CLP load cell (HBM, Darmstadt, Germany) was used to measure the uni-axial tension force of the applied load. Displacement, which was caused by the screw, was measured from the initial distance to the flexible part.

#### 2.4. Surface Analysis

The surfaces of NiTi orthodontic archwires after simulation testing were examined with scanning electron microscopy (SEM, Sirion 400 NC, FEI, Hillsboro, OR, USA) and auger electron spectroscopy (AES). The initial (non-deformed and non-immersed) orthodontic archwire served as a control. AES was performed while using a Microlab 310F VG-Scientific SEM/AES/X-ray photoelectron spectroscopy (XPS) (Thermo Scientific, Waltham, MA, USA), a field emission scanning spectrometer of auger electrons. A 10 kV primary electron beam was employed for this investigation, with a primary electron beam current of approximately 10 nA and approximate diameter of 10 nm resolution. The sample was Ar<sup>+</sup> sputtered with a sputter rate of 1 nm/min. for different sputter length times. AES spectrum was made after each sputtering time [35].

#### 2.5. Measurement of Ions' Release

We prepared two types of testing in order to determine the impact of the load simulation on the release of ions from NiTi archwire in CACO-2 cell culture medium: (i) Exposure of NiTi archwires without any loading i.e., only immersed for 24 h (as a control sample) and (ii) Exposure with SMAS loading under the same conditions (four archwires, the same volume of medium, temperature, etc.). Inductively coupled plasma mass spectrometry (ICP-MS) while using a spectrometer (HP, Agilent 7500 ce, equipped with a collision cell, Santa Clara, CA, USA), was performed on both CACO-2 cell culture mediums to measure the concentration of the released nickel and titanium ions. ICP-MS analysis was carried out under the operating conditions: Power = 1.5 kW, Nebulizer = Meinhard, plasma gas flow (L/min) = 15, Nebulizer gas flow (L/min) = 0.85, Make up gas flow (L/min) = 0.28, and Reaction gas flow (mL/min) = 4.0. Prior to the analysis, the samples were dissolved in 10% (v/v) aqua regia. Matrix matched calibration solutions were prepared and analysed for calibration. Relative measurement uncertainty was established to be ±3%. The ICP-MS technique was used due to the advantages over other elemental analysers, as it is possible to perform quantitative analysis in a very large concentration range (from ng/mL in the sample solution until 100% in the sample). Besides this, correlation between the signal and concentration is linear for about five orders of magnitude for most of the analyses; there is a relatively good precision of measurements (around 3%), low matrix effects, and short analysis time.

### 3. Results and Discussion

#### 3.1. Surface Analysis

The surface examination with SEM showed significant microstructure differences between the initial and deformed archwires (see Figure 3a,b). The initial archwire surface is rough, with visible holes and other defects, while the deformed archwire surface is smooth and without any other visible defects (inclusions, etc.). This can be attributed to the influence of mechanical loading, which led to the elongation and permanent deformation of the NiTi archwire [36] and the faster release of elements from the surface into the medium.

AES analyses were performed on the selected archwire surfaces (A1, A2—Figure 3a,b), the results are shown in Figure 4a,b. The AES detected a signal from the carbon, mostly originating from the C–C bonds at 280 eV, which suggested a residual contamination, probably from the atmosphere. Analysis of the spectra in the Ti 2*p* region indicates all the titanium to be present in the form of TiO<sub>2</sub>. It has binding energies at 380 and 420 eV. The signal from the Ni 2*p* region was dominated by one large peak at 850 eV in both wires, but it is larger in the second deformed wire. There are also two smaller peaks at 730 and 780 eV that are similar in both of the wires. They correspond to the nickel oxides NiO and Ni<sub>2</sub>O<sub>3</sub>. The peak at 850 eV corresponds to elemental nickel. In Figure 4b, oxygen had one peak at approximately 530 eV, which pointed to a significant contribution from the Ti oxide, and upon closer inspection, another peak is observable at approximately 500 eV, which corresponds to Ni oxide. The deformed wire showed a higher level of nickel oxide at 500 eV despite the small amount of Ni oxide in the control wire.



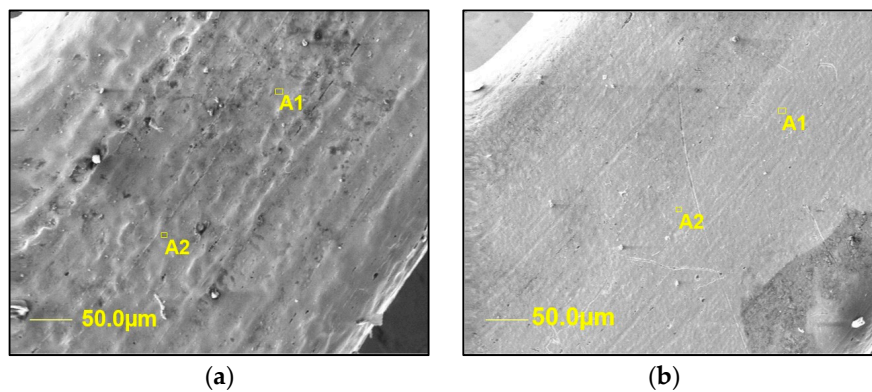


**Figure 3.** SEM image of: (a) Initial archwire surface (control); (b) Deformed archwire surface after the simulation of multiaxial stress equipment (SMAS) simulation test.

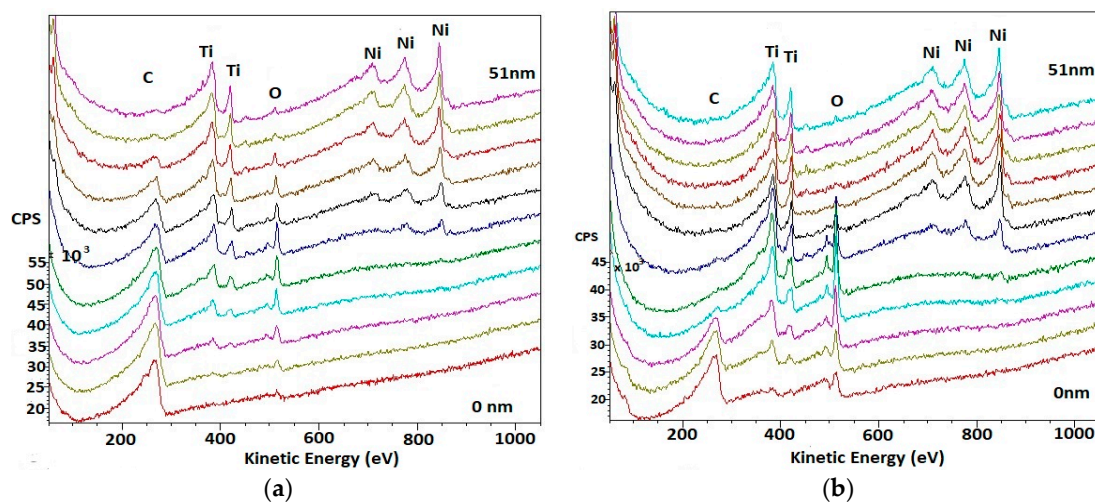


**Figure 4.** Auger electron spectroscopy (AES) spectra of archwire surfaces: (a) Initial (control); (b) Deformed after the SMAS simulation test.

Surface analysis AES showed concentration of elements in the first 51 nm of the selected archwires—Figure 5a,b depicts those results and discovered different concentrations of elements between the initial and deformed archwires. AES revealed the presence of carbon on the surface of both archwires. The binding energy of the carbon shows that it originates from the atmosphere (Figure 4a,b). It was detected that there is 40% less carbon present in the deformed archwire in 4 nm of depth, and an almost undetectable amount from 10 nm of depth, although, oxygen replaces carbon in the superficial layer of the wire in the deformed archwire (Figure 5b). Titanium is present on the surface of both archwires, and the nickel content is undetectable in the first 4 nm of both archwires. Therefore, it can be concluded that the oxygen is evidently connected to titanium, forming a protective layer of titanium oxides. In contrast to nickel, titanium with oxygen reacts immediately, and it forms a few oxides, but the most stable is in the form of  $\text{TiO}_2$ . The thickness of the oxide layer in the deformed archwire is about 51 nm, which is concluded from the fact that the level of oxygen drops to a concentration of 0% (Figure 5b). That is in accordance with the finding that the Ti-oxide film thickness ranges between 7 and 70 nm [37]. In contrast to this, the oxide layer is much thicker in the initial archwire, and the concentration of oxygen at a depth of 51 nm was still 12.2% (Figure 5a). The precise thickness of the oxide layer could not be detected on the initial archwire due to the fact that the AES was performed in the first 51 nm of the surface. Therefore, it could be concluded that the deformation of the archwire during 24 h affected the oxide thickness. The oxygen content of the deformed archwire differs from the initial archwire, and it is the highest at a depth of 6 nm. From Figure 4a,b it can be predicted that there is a significantly higher content of nickel oxide in the deformed archwire. The content of

the nickel oxide is noticeable between 4 and 11 nm of the deformed archwire. From the results that were obtained, the amount of titanium is constantly increasing towards the bulk of the material in both archwires, and thus the amount of nickel shows a similar pattern in the initial archwire. However, this is slightly altered in the deformed archwire, where the rapid increase of nickel concentration can be noticed from the 11 nm depth. The difference of the nickel content is more than double at 16 nm depth between the archwires. From Figure 4b it can be concluded that most of the reason for that increased nickel content is in its elemental and oxidised state, which explains the phenomenon that, during the deformation of the archwire, nickel ions diffuse from the bulk of the material to the surface layer. Importantly, surface nickel ions dissolve more easily into the environment, similar to nickel ions during the heat treatment process that was described by Shabalovskaya et al. [33]. Besides oxide thickness, the surface nickel concentration in NiTi shape memory alloys is a very important factor when considering the stability of the archwires [37]. The deformed archwire also exhibits a significant release of Ni ions due to the change in Ni/Ti ratio in contrast to the initial archwire. This is also followed by a thinner C-adsorption layer, which prevents the opening of the cracks in the Ti-oxide layer and the dissolution of Ni ions into the CACO-2 cell culture medium.

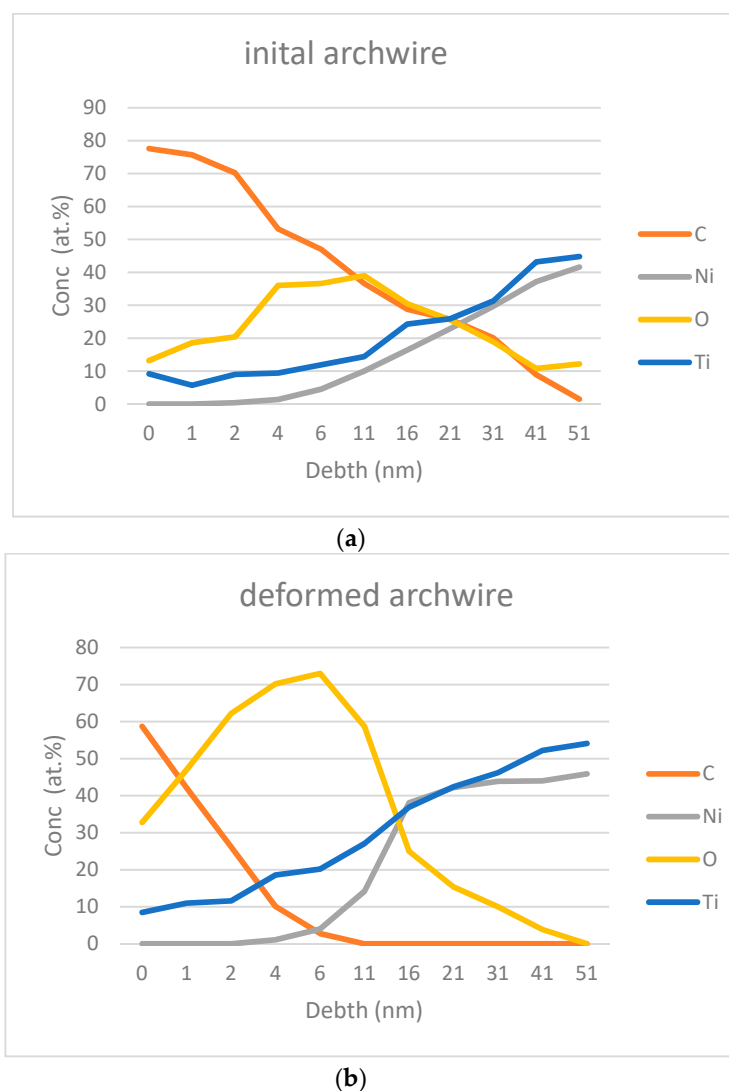


**Figure 5.** AES depth profiles show the concentrations of elements in the direction from the surface to 51 nm in the depth of each of the archwires: (a) Initial (control), (b) Deformed after the SMAS simulation test.

### 3.2. Results of Ions' Release

Table 1 shows the ICP-MS results of the ions' release in the CACO-2 cell culture mediums. The results indicated that titanium concentrations are below the detection limit ( $<0.05 \mu\text{g/L}$ ) in both of the samples. On the other hand, the concentration of nickel is different; the difference was  $70 \mu\text{g/L/day}$ . This suggested a small level of nickel leakage out of the archwire into the media.

**Table 1.** Ni and Ti ion concentrations from NiTi archwire in CACO-2 cell culture mediums after exposure with without loading (as a control sample) and after SMAS testing.

Sample	Conc Ni ( $\mu\text{g/L}$ )	Conc Ti ( $\mu\text{g/L}$ )
Control	1.240	$<0.05$
SMAS Testing	1.310	$<0.05$

Based on the obtained results, it can be concluded that the deformation of the archwire is an important factor that increases nickel release into the CACO-2 cell culture media. The concentration of nickel is  $70 \mu\text{g/L}$  higher after 24 h in comparison with an unloaded archwire. Moreover, this represents the mean level of nickel released from a single wire of the average length of 12 cm (four pieces), while the patients usually have two arch wires in their mouth, and thus a total value of  $140 \mu\text{g/L}$  additional nickel release. These results are in correlation with the literature, where similar levels of Ni release from similar archwires are mentioned during a comparable period of time [38,39]. The shape of the archwire can also influence the amount of nickel released, and rectangular archwires release more elements than round ones [40]. The value of released nickel is below the daily dietary intake level ( $300\text{--}500 \mu\text{g}$ ) [41] and below the critical results (it must be taken into account that nickel can be released from a whole orthodontic appliance, which consists of bands, brackets, or some other attachments that also increase the nickel levels in the mouth). The physiological values are, therefore, much higher, and they can sometimes cause allergic reactions [42]. Furthermore, one study showed that even sub-toxic concentrations of metal ions can alter osteoblast activity [43]. Similarly, other authors [44] demonstrated that the  $7.2 \text{ g/mL}$  Ni ions released were sufficient for stimulating monocyte secretion of IL1, which, consequently, promoted endothelial cells to induce ICAM1 indirectly (Intracellular adhesion molecules that are involved in the activation of other Inflammatory cells). In addition, Cederbrant et al. [45] showed that an increase in lymphocyte proliferation and IL1 secretion could be induced, even with a small quantity of nickel, which is in correlation with our previous finding that thought archwires were non-cytotoxic for L929 cells, according to ISO Standards [15841:2014] [46], Rematitan superelastic archwires induced the apoptosis of rat thymocytes. This finding suggests strongly that, besides the released nickel ion concentration, the surface of the NiTi wire is most probably responsible for the cytotoxic effect [38]. It is important to declare that, in clinical conditions, orthodontic archwires are subjected to additional masticatory forces, abrasive forces from food and toothbrushes, and also temperature changes and various chemicals from saliva, liquids, and medicine. These can all damage the protective surface titanium oxide layer and cause corrosion, which leads to an increased level of released nickel ions. A few studies concluded that saliva, probiotic supplement and oral antiseptics affect both the general and localised corrosion of NiTi archwires, which also affects the mechanical properties and the release of nickel from NiTi archwires [47,48]. The oral environment is harsh and the conditions can change every second, so the archwires that are placed in the mouth need to resist all of those changes, including corrosion. Sometimes orthodontic treatment is complex [49,50] and the forces that are produced are much stronger than the ones with an average patient. Due to this complex situation, it is difficult to simultaneously simulate all of those conditions during in vitro studies.

It is necessary to improve the surface as a research challenge, and for safe use of NiTi archwires in the future. Namely, the presented study showed that the release of nickel ions from NiTi archwires is not negligible. According to the literature, it is known that one possible way could be nitriding of titanium with the formation of TiN/TiN<sub>2</sub>, as nitrogen has a higher hardening effect than oxygen [51,52].



The other possible option could be the application of different coatings onto the NiTi surface that can improve its characteristics [53]. From other studies it was found out that there are good results in improving the frictional, biological, and aesthetic properties of stainless steel with electrophoretic deposition of a bioactive glass coating that could also be implemented on NiTi archwires [54].

#### 4. Conclusions

Within the present study of NiTi orthodontic archwires' simulation loaded with multiaxial stresses in CACO2-2 cell culture, specific conclusions could be drawn.

The deformation of the NiTi archwire up to 30° during 24 h is enough to produce surface structural changes. SEM investigations of the deformed archwire surface revealed evident modification in the roughness, and the surface became smoother. On this surface, 40% less carbon was detected in comparison with the initial archwire surface. Besides this, the formatted thickness of the oxide layer on the surface was about 51 nm, while this could not be detected in the case of the initial archwire surface. It was found out that deformation accelerates the formation of oxides on the surface and with this oxide thickness, where a significantly higher content of nickel oxide was detected in the depth between 4 and 11 nm below the archwire surface. The oxygen content of the deformed archwire surface differed from the initial archwire surface, and it reached the highest value at a depth of 6 nm. This could be attributed to the phenomenon that, during the deformation of the archwire, nickel ions diffused faster from the bulk of the archwire surface.

Measurable nickel release during SMAS simulation of an archwire 12 cm in length is 1.310 µg/L, even after short period of 24 h. These data could be important for clinical orthodontic praxis. Additionally, the next studies must investigate the deformation time of the archwires, when considering the fact that NiTi orthodontic archwires could be in the oral environment for months, which can have considerable clinical implications. Based on the obtained results, it is recommended that, also in the case of biocompatibility, studies must be conducted to investigate the influence of archwire loading on the possible increase of nickel release content in comparison with the existing tests in order to obtain the most realistic information regarding surface stability.

**Author Contributions:** Conceptualization, R.R. and N.L.; Methodology, I.Š., B.G. and R.R.; Software, N.L., Validation, N.L., I.Š., B.G. and R.R.; Formal Analysis, M.J., M.G. and S.H.; Investigation, N.L., R.R., M.J., M.G. and S.H.; Writing—Original Draft Preparation, N.L. and R.R.; Writing—Review and Editing, R.R.; Funding Acquisition, I.Š., B.G., M.J. and R.R.

**Funding:** This research was funded by the Slovenian Research Agency ARRS (I0-0029—Infrastructure program University of Maribor) and by Eureka program ORTO-NITI E!6788 funded by Ministry of Education, Science and Technological Development Republic of Serbia.

**Acknowledgments:** The responsible proof reader for the English language is Shelagh Hedges, Faculty of Mechanical Engineering, University of Maribor, Slovenia.

**Conflicts of Interest:** The authors declare no conflict of interest.

#### References

1. Sidebottom, A.J.; Mistry, K. Prospective analysis of the incidence of metal allergy in patients listed for total replacement of the temporomandibular joint. *Br. J. Oral Maxillofac. Surg.* **2014**, *52*, 85–86. [[CrossRef](#)] [[PubMed](#)]
2. Dunlap, C.L.; Vincent, S.K.; Barker, B.F. Allergic reaction to orthodontic wire: Report of case. *J. Am. Dent. Assoc.* **1989**, *118*, 449–450. [[CrossRef](#)] [[PubMed](#)]
3. Al-Waheidi, E.M.H. Allergic reaction to nickel orthodontic wires: A case report. *Quintessence Int.* **1995**, *26*, 385–387. [[PubMed](#)]
4. Bass, J.K.; Fine, H.; Cisneros, G.J. Nickel hypersensitivity in the orthodontic patient. *Am. J. Orthod. Dentofacial Orthop.* **1993**, *103*, 280–285. [[CrossRef](#)]
5. Dass, K.; Buchner, V. Effects of nickel exposure on peripheral tissues: role of oxidative stress in toxicity and possible protection by ascorbic acid. *Rev. Environ. Health* **2007**, *22*, 157–173. [[CrossRef](#)]

6. Valko, M.; Morris, H.; Cronin, M.T. Metals toxicity and oxidative stress. *Curr. Med. Chem.* **2005**, *12*, 1161–1208. [[CrossRef](#)] [[PubMed](#)]
7. M'Bemba-Meka, P.; Lemieux, N.; Chakrabarti, S.K. Role of oxidative stress, mitochondrial membrane potential and calcium homeostasis in human lymphocyte death induced by nickel carbonate hydroxide in vivo. *Arch. Toxicol.* **2006**, *80*, 405–420. [[CrossRef](#)] [[PubMed](#)]
8. Dieter, M.P.; Jameson, C.W.; Tucker, A.N.; Luster, M.I.; French, J.E.; Hong, H.L.; Boorman, G.A. Evaluation of tissue deposition myelopoietic and immunologic responses in mice after long term exposure to nickel sulfare in drinking water. *J. Toxicol. Environ. Health* **1988**, *24*, 357–372. [[CrossRef](#)]
9. Hostynek, J.J. Sensitization to nickel: etiology, epidemiology, immune reactions, prevention and therapy. *Rev. Environ. Health* **2006**, *21*, 252–280. [[CrossRef](#)]
10. Liang, R.; Senturker, S.; Shi, X.; Bal, W.; Dizdaro-gluand, M.; Kasprzak, K.S. Effects of Ni (II) and Cu (II) on DNA interactions with the N-terminal sequence of human protamine P2: Enhancement of binding and mediation of oxidative DNA strand scission and base damage. *Carcinogenesis* **1999**, *20*, 893–898. [[CrossRef](#)]
11. Kasprzak, K.S.; Sunderman, F.W.J.; Salnikow, K. Nickel carcinogenesis. *Mutat. Res.* **2003**, *533*, 67–97. [[CrossRef](#)] [[PubMed](#)]
12. Rahilly, G. Nickel allergy and orthodontics. *J. Orthod.* **2003**, *30*, 171–174. [[CrossRef](#)] [[PubMed](#)]
13. Huang, H.H.; Chiu, Y.H.; Lee, T.H.; Wu, S.C.; Yang, H.W.; Su, K.H.; Hsu, C.C. Ion release from NiTi orthodontic wires in artificial saliva with various acidities. *Biomaterials* **2003**, *24*, 3585–3592. [[CrossRef](#)]
14. Ryhanen, J.; Niemi, E.; Serlo, W.; Niemela, E.; Sandvik, P.; Pernu, H.; Salo, T. Biocompatibility of nickel-titanium shape memory metal and its corrosion behavior in human cell cultures. *J. Biomed. Mater. Res.* **1997**, *35*, 451–457. [[CrossRef](#)]
15. Chan, C.; Trigwell, C.; Duerig, T. Oxidation of a NiTi alloy. *Surf. Interface Anal.* **1990**, *15*, 349–354. [[CrossRef](#)]
16. Espinos, J.P.; Fernandes, A.; Gonzales-Elipe, A.R. Oxidation and diffusion processes in nickel-titanium oxide systems. *Surf. Sci.* **1993**, *295*, 402–410. [[CrossRef](#)]
17. Heravi, F.; Moayed, M.H.; Mokhber, N. Effects of fluoride on nickel-titanium and stainless-steel orthodontic archwires: An in vitro study. *J. Dent.* **2015**, *12*, 49–59.
18. Qu, J.; Blau, P.J.; Watkins, T.R.; Cavin, O.B.; Kulkarni, N.S. Friction and wear of titanium alloys sliding against metal, polymer and ceramic counterfaces. *Wear* **2005**, *258*, 1348–1356. [[CrossRef](#)]
19. Zhenping, S.; Jiqiang, W.; Zhengbin, W.; Yanxin, Q.; Tianying, X.; Yugui, Z. Cavitation erosion and jet impingement erosion of the NiTi coating produced by air plasma spraying. *Coatings* **2018**, *8*, 346.
20. Freiberg, K.E.; Bremer-Streck, S.; Kiehnopf, M.; Rettenmayr, M.; Undisz, A. Effect of thermomechanical pre-treatment on short- and long-term Ni release from biomedical NiTi. *Acta Biomater.* **2014**, *10*, 2290–2295. [[CrossRef](#)]
21. Jia, W.; Beatty, M.W.; Reinhardt, R.A.; Petro, T.M.; Cohen, D.M.; Maze, C.R.; Strom, E.A.; Hoffman, M. Nickel release from orthodontic arch wires and cellular immune response to various nickel concentrations. *J. Biomed. Mater. Res.* **1999**, *48*, 488–495. [[CrossRef](#)]
22. Chieruzzi, M.; Pagano, S.; Cianetti, S.; Lombardo, G.; Kenny, J.M.; Torre, L. Effect of fibre post, bone losses and fibre content on the biomechanical behaviour of endodontically treated teeth: 3D-finite element analysis. *Mater. Sci. Eng. C* **2017**, *74*, 334–346. [[CrossRef](#)] [[PubMed](#)]
23. Fercec, J.; Anzel, I.; Rudolf, R. Stress dependent electrical resistivity of orthodontic wire from the shape memory alloy NiTi. *Mater. Des.* **2014**, *55*, 699–706. [[CrossRef](#)]
24. Vázquez-Sánchez; Ángeles, M. Available online: <https://readycell.com/cacoready/> (accessed on 19 July 2018).
25. Calabro, A.R.; Gazarian, D.I.; Barile, F.A. Effect of metals on  $\beta$ -actin and total protein synthesis in cultured human intestinal epithelial cells. *J. Pharmacol. Toxicol. Methods* **2011**, *63*, 47–58. [[CrossRef](#)] [[PubMed](#)]
26. Richter, J.W.; Shull, G.M.; Fountain, J.H.; Guo, Z.; Musselman, L.P.; Fiumera, A.C.; Mahler, G.J. Titanium dioxide nanoparticle exposure alters metabolic homeostasis in a cell culture model of the intestinal epithelium and drosophila melanogaster. *Nanotoxicology* **2018**, *12*, 390–406. [[CrossRef](#)] [[PubMed](#)]
27. García-Rodríguez, A.; Vila, L.; Cortés, C.; Hernández, A.; Marcos, R. Effects of differently shaped TiO<sub>2</sub>NPs (nanospheres, nanorods and nanowires) on the in vitro model (Caco-2/HT29) of the intestinal barrier. *Part. Fibre Toxicol.* **2018**, *15*, 33. [[CrossRef](#)] [[PubMed](#)]
28. Staffolani, N.; Damiani, F.; Lilli, C.; Guerra, M.; Staffolani, N.J.; Belcastro, S.; Locci, P. Ion release from orthodontic appliances. *J. Dent.* **1999**, *27*, 449–454. [[CrossRef](#)]

29. Cisse, O.; Savagodo, O.; Wu, M.; Yahia, L. Effect of surface treatment of NiTi alloy on its corrosion behavior in Hanks solution. *J. Biomed. Mater. Res.* **2002**, *61*, 339–345. [[CrossRef](#)]
30. Kobayashi, S.; Ohgoe, Y.; Ozeki, K.; Sato, K.; Sumiya, T.; Hirakuri, K. Diamond-like carbon coatings on orthodontic archwires. *Diam. Relat. Mater.* **2005**, *14*, 1094–1097. [[CrossRef](#)]
31. Sui, J.; Cai, W. Effect of diamond-like carbon (DLC) on the properties of NiTi alloys. *Diam. Relat. Mater.* **2006**, *15*, 1720–1726. [[CrossRef](#)]
32. Clarke, B.; Carroll, W.; Rochev, Y.; Hynes, M.; Bradley, D.; Plumley, D. Influence of nitinol wire surface treatment on oxide thickness and composition and its subsequent effect on corrosion resistance and nickel ion release. *J. Biomed. Mater. Res. A* **2006**, *79*, 61–70. [[CrossRef](#)] [[PubMed](#)]
33. Shabalovskaya, S.; Anderegg, J.; Laab, F.; Thiel, P.A.; Rondelli, G. Surface conditions of Nitinol wires, tubing, and as-cast alloys. The effect of chemical etching, aging in boiling water, and heat treatment. *J. Biomed. Mater. Res.* **2003**, *65B*, 193–203. [[CrossRef](#)] [[PubMed](#)]
34. Pagano, S.; Chieruzzi, M.; Balloni, S.; Lombardo, G.; Torre, L.; Bodo, M.; Cianetti, S.; Mairnucci, L. Biological, thermal and mechanical characterization of modified glass ionomer cements: The role of nanohydroxyapatite, ciprofloxacin and zinc L-carnosine. *Mater. Sci. Eng. C* **2019**, *94*, 76–85. [[CrossRef](#)] [[PubMed](#)]
35. Shabalovskaya, S.; Anderegg, J. Surface spectroscopic characterization of TiNi nearly equiatomic shape memory alloys for implants. *J. Vac. Sci. Technol. A* **1995**, *13*, 2624–2632. [[CrossRef](#)]
36. Uchil, J.; Mahesh, K.K.; Ganesh-Kumara, K. Electrical resistivity and strain recovery studies on the effect of thermal cycling under constant stress on R-phase in NiTi shape memory alloy. *Phys. B Condens. Mater.* **2002**, *324*, 419–428. [[CrossRef](#)]
37. Shabalovskaya, S.A. On the nature of the biocompatibility and medical applications of NiTi shape memory and superelastic alloys. *Biomed. Mater. Eng.* **1996**, *6*, 267–289. [[PubMed](#)]
38. Colic, M.; Tomic, S.; Rudolf, R.; Markovic, E.; Scepan, I. Differences in biocompatibility, dynamics of the oxide layers' formation, and nickel release between superelastic and thermo-elastic activated nickel-titanium archwires. *J. Mater. Sci. Mater. Med.* **2016**, *27*, 128.
39. Ramazanzadeh, B.A.; Ahrari, F.; Sabzevari, B.; Habibi, S. Nickel ion release from three types of nickel-titanium-based orthodontic archwires in the as-received state and after oral simulation. *J. Dent. Res. Dent. Clin. Dent. Prospects* **2014**, *8*, 71–76.
40. Azizi, A.; Jamilian, A.; Nucci, F.; Kamali, Z.; Hosseinihoo, N.; Perillo, L. Release of metal ions from round and rectangular NiTi wires. *Prog. Orthod.* **2016**, *17*, 10. [[CrossRef](#)]
41. Schroeder, H.A.; Balassa, J.J.; Tipton, I.H. Abnormal trace metals in man-nickel. *J. Chron. Dis.* **1962**, *15*, 51–65. [[CrossRef](#)]
42. Kaaber, K.; Veien, N.K.; Tjell, J.C. Low nickel diet in the treatment of patients with chronic nickel dermatitis. *Br. J. Dermatol.* **1978**, *98*, 197–201. [[CrossRef](#)] [[PubMed](#)]
43. Sun, Z.L.; Wataha, C.T.; Hanks, C.T. Effects of metal ions on osteoblast-like cell metabolism and differentiation. *J. Biomed. Mater. Res.* **1997**, *34*, 29–37. [[CrossRef](#)]
44. Wataha, J.C.; Lockwood, P.E.; Marek, M.; Ghazi, M. Ability of Ni-containing biomedical alloys to activate monocytes and endothelial cells in vitro. *J. Biomed. Mater. Res.* **1999**, *45*, 251–257. [[CrossRef](#)]
45. Cederbrant, K.; Anderson, C.; Andersson, T.; Marcusson-Stahl, M.; Hultman, P. Cytokine production, lymphocyte proliferation and T-cell receptor V $\beta$  expression in primary peripheral blood mononuclear cell cultures from nickel-allergic individuals. *Int. Arch. Allergy Immunol.* **2003**, *132*, 373–379. [[CrossRef](#)] [[PubMed](#)]
46. ISO 15841:2014: *Dentistry—Wires for Use in Orthodontics*; International Organization for Standardization: Geneva, Switzerland, 2014.
47. Rincic Mlinaric, M.; Karlovic, S.; Ciganj, Z.; Acev, D.P.; Pavlic, A.; Spalj, S. Oral antiseptics and nickel-titanium alloys: Mechanical and chemical effects of interaction. *Odontology* **2019**, *107*, 150–157. [[CrossRef](#)] [[PubMed](#)]
48. Trolić, I.M.; Turco, G.; Contardo, L.; Serdarević, N.L.; Ćurković, H.O.; Špalj, S. Corrosion of nickel-titanium orthodontic archwires in saliva and oral probiotic supplements. *Acta Stomatol. Croat.* **2017**, *51*, 316–325.
49. D'Attilio, M.; Rodolfo, D.; Filippakos, A.; Saccucci, M.; Festa, F.; Tripodi, D. Second class resolver: A retrospective analysis. *Eur. J. Paediatr. Dent.* **2014**, *15*, 78–82.
50. Baldini, A.; Nota, A.; Santariello, C.; Assi, V.; Ballanti, F.; Gatto, R.; Cozza, P. Sagittal dentoskeletal modifications associated with different activation protocols of rapid maxillary expansion. *Eur. J. Paediatr. Dent.* **2018**, *19*, 151–155.

51. Kamat, A.M.; Copley, S.M.; Segal, A.E.; Todd, J.A. Laser-sustained plasma (LSP) nitriding of titanium: A review. *Coatings* **2019**, *9*, 283. [[CrossRef](#)]
52. Al Jabbari, Y.S.; Fehrman, J.; Barnes, A.C.; Zapf, A.M.; Zinelis, S.; Berzins, D.W. Titanium nitride and nitrogen ion implanted coated dental materials. *Coatings* **2012**, *2*, 160–178. [[CrossRef](#)]
53. Arango, S.; Peláez-Vargas, A.; García, C. Coating and surface treatments on orthodontic metallic materials. *Coatings* **2013**, *3*, 1–15. [[CrossRef](#)]
54. Kawaguchi, K.; Iijima, M.; Endo, K.; Mizoguchi, I. Electrophoretic deposition as a new bioactive glass coating process for orthodontic stainless steel. *Coatings* **2017**, *7*, 199. [[CrossRef](#)]



© 2019 by the authors. Licensee MDPI, Basel, Switzerland. This article is an open access article distributed under the terms and conditions of the Creative Commons Attribution (CC BY) license (<http://creativecommons.org/licenses/by/4.0/>).